



**HAL**  
open science

## Intercomparison exercise on difficult to measure radionuclides in activated concrete - Statistical analysis and comparison with activation calculations

Anumaija Leskinen, Céline Gautier, Antti Rätty, Tommi Kekki, Elodie Laporte, Margaux Giuliani, Jacques Bubendorff, Julia Laurila, Kristian Kurhela, Pascal Fichet, et al.

### ► To cite this version:

Anumaija Leskinen, Céline Gautier, Antti Rätty, Tommi Kekki, Elodie Laporte, et al.. Intercomparison exercise on difficult to measure radionuclides in activated concrete - Statistical analysis and comparison with activation calculations. *Journal of Radioanalytical and Nuclear Chemistry*, 2021, 10.1007/s10967-021-07824-7 . cea-03783338

**HAL Id: cea-03783338**

**<https://cea.hal.science/cea-03783338>**

Submitted on 22 Sep 2022

**HAL** is a multi-disciplinary open access archive for the deposit and dissemination of scientific research documents, whether they are published or not. The documents may come from teaching and research institutions in France or abroad, or from public or private research centers.

L'archive ouverte pluridisciplinaire **HAL**, est destinée au dépôt et à la diffusion de documents scientifiques de niveau recherche, publiés ou non, émanant des établissements d'enseignement et de recherche français ou étrangers, des laboratoires publics ou privés.

1           **Intercomparison exercise on difficult to measure**  
2           **radionuclides in activated concrete - statistical analysis**  
3           **and comparison with activation calculations**

4           Anumaija Leskinen<sup>1\*</sup>, Celine Gautier<sup>2</sup>, Antti Rätty<sup>1</sup>, Tommi Kekki<sup>1</sup>, Elodie Laporte<sup>2</sup>,  
5           Margaux Giuliani<sup>2</sup>, Jacques Bubendorff<sup>2</sup>, Julia Laurila<sup>3,4</sup>, Kristian Kurhela<sup>3,4</sup>, Pascal  
6           Fichet<sup>2</sup>, Susanna Salminen-Paatero<sup>3</sup>

7           <sup>1</sup>*Technical Research Centre of Finland, Kivimiehentie 3, 02044 VTT, Finland*

8           <sup>2</sup>*Des-Service d'Etudes Analytiques et de Reactivite des Surfaces (SEARS), CEA,*  
9           *Université Paris-Saclay, F91191 Gif Sur Yvette, France*

10          <sup>3</sup>*Department of Chemistry, Radiochemistry, A.I. Virtasen aukio 1, P.O. Box 55, FI-00014*  
11          *University of Helsinki, Finland*

12          <sup>4</sup>*Metropolia University of Applied Sciences, P.O. Box 4071,*  
13          *00079 Metropolia, Finland*

15          **Abstract**

16          This paper reports the results obtained in a Nordic Nuclear Safety Research (NKS) project  
17          during the second intercomparison exercise for the determination of difficult to measure  
18          (DTM) radionuclides in decommissioning waste. Eight laboratories participated by  
19          carrying out radiochemical analysis of <sup>3</sup>H, <sup>14</sup>C, <sup>36</sup>Cl, <sup>41</sup>Ca, <sup>55</sup>Fe and <sup>63</sup>Ni in an activated  
20          concrete. In addition, gamma emitters, namely <sup>152</sup>Eu and <sup>60</sup>Co, were analysed. The assigned  
21          values were derived from the submitted results according to ISO 13528 standard and the

---

\* corresponding author

22 performance assessments were determined using z scores. The measured results were  
23 compared with activation calculation result showing varying degree of comparability.

## 24 **Keywords**

25 Difficult to measure radionuclides, intercomparison exercise, decommissioning waste,  
26 concrete, biological shield, ISO 13528

## 27 **Introduction**

28 A three-year intercomparison exercise project within Nordic Nuclear Safety Research  
29 (NKS) community on radiochemical analysis of difficult to measure (DTM) radionuclides  
30 in decommissioning waste began in 2019. The first year intercomparison exercise results  
31 on DTM analyses in an activated steel were published by Leskinen et al. [1,2]. This paper  
32 presents the results of the second year intercomparison exercise, which was carried out on  
33 analysis of DTMs in an activated concrete. Similar to the first year, eight laboratories  
34 participated; three from Finland, one from Sweden, two from Norway, one from Denmark,  
35 and one from France. The focus was on determination of  $^3\text{H}$ ,  $^{14}\text{C}$ ,  $^{55}\text{Fe}$  and  $^{63}\text{Ni}$  whereas  
36  $^{36}\text{Cl}$  and  $^{41}\text{Ca}$  were optional. In addition to DTMs, the key gamma emitters present in the  
37 activated concrete, namely  $^{152}\text{Eu}$  and  $^{60}\text{Co}$ , were measured. The results were analysed  
38 according to the ISO 13528 standard [3], which enabled statistical analysis of the submitted  
39 results using robust methods. The samples were determined to be homogenous and the  
40 assigned values were derived from the submitted results according to the ISO 13528  
41 standard. The overall procedure was presented in the NKS report series [4] whereas in this  
42 paper, the results are further analysed and compared with activation calculation results.  
43 The studied activated concrete originated from FiR1 research reactor biological shield, for  
44 which the chemical composition, irradiation history and cooling time had been studied  
45 previously [5]. The calculated activity concentration results were derived using a  
46 combination of a MCNP neutron flux model [10] and a point kinetic code ORIGEN-S [6].  
47 Preliminary activation calculation results on the DTM activity concentrations and chemical  
48 composition results were provided to the participants prior to the analysis phase. As such,

49 low activity concentrations were expected. This paper discusses the final activation  
50 calculation results and compares them with the measured activity concentration results.  
51 Discussion on the limit of detection (LOD) and uncertainty calculations among the  
52 participating laboratories are also presented.

### 53 **Sample history, homogeneity and stability**

54 The studied activated concrete originated from the biological shield of 250kW FiR1  
55 TRIGA Mark II research reactor. FiR1 was the first nuclear reactor in Finland serving over  
56 50 years in education, research, isotope production, and cancer treatment. The reactor was  
57 shut down permanently in 2015 and the dismantling is expected to begin in 2022.  
58 Characterisation of the FiR1 activated components has been carried out using both  
59 modelling and experimental studies [7-9]. Experimental characterisation of the biological  
60 shield began in 2014 with coring of inactive concrete cores to which, for example, testing  
61 of mechanical properties and chemical composition analyses were carried out. The results  
62 concluded that the concrete contained different types of stones mainly up to 32 mm, but  
63 also up to 80 mm diameter making the material quite heterogeneous in small scale. The  
64 chemical compositions of elements of interest determined in the inactive concrete core  
65 samples are presented in Table 1. The characterisation studies continued in 2018 when  
66 three activated concrete cores were taken from the activated part of the biological shield.  
67 The physical locations of the activated concrete cores were at different height and side of  
68 the biological shield compared to the inactive concrete cores. A separate article describing  
69 the calculation model and comparison between calculated and measured gamma activity  
70 concentrations in the cores as a function of distance from the irradiation source is under  
71 preparation by the corresponding affiliation. For this study, the most activated concrete  
72 core was sampled by drilling, which produced fine powder. The drilling procedure will be  
73 presented in an upcoming publication by the corresponding author. Due to the presence of  
74 different types and sizes of stones, a large sample size (approximately 180 g) was  
75 considered to produce a representative sample. Additionally, small grain size was expected  
76 to be easier for acid digestion due to a larger surface area. The drilled powder was mixed  
77 and 20 g was weighed into eight glass liquid scintillation vials. The homogeneity

78 measurements were carried out according to the ISO 13528 standard section 6.1  
 79 “Homogeneity and stability of proficiency test items and Annex B” [3]. The homogeneity  
 80 measurand was  $^{152}\text{Eu}$  activity concentration, because it was easy to measure as a gamma  
 81 emitter and it had highest abundance in the samples. The measurements were carried out  
 82 using a p-type HPGe semiconductor detector with 18% relative efficiency (ISOCS  
 83 Canberra Ltd connected with Inspector 2000 multichannel analyser and Genie 2000  
 84 software). Geometry Composer v.4.4 was utilised for efficiency calibrations. The density  
 85 of the drilled concrete, which is one of the parameters needed in the efficiency calculations,  
 86 was calculated from the mass and volume of the samples. Each sample was carefully  
 87 positioned on top of the detector in order to obtain a constant measurement geometry. The  
 88 measurement time was 10800 s. All samples were measured twice and the homogeneity  
 89 was assessed using Eq. (1) as presented in the ISO 13528 standard. The  $s_s$  of the Eq. (1)  
 90 was calculated from sample averages, between-test-portion ranges, general average,  
 91 standard deviation of sample averages, within-sample deviation and between-sample  
 92 standard deviation (equations presented in Annex B of the ISO 13528 standard). However,  
 93 because  $\sigma_{pt}$  e.g. robust standard deviation of participant results was not known at the  
 94 beginning of the project, relative standard deviation (RSD) of  $^{152}\text{Eu}$  results (average  
 95  $19.7 \pm 0.3 \text{ Bq g}^{-1}$ ) was estimated to represent homogeneity. As the RSD was 1.7%, the  
 96 samples were considered homogenous. At the end of the project, when the  $\sigma_{pt}$  was  
 97 calculated from the submitted results, Eq. (1) was calculated to be true and therefore, the  
 98 samples were homogenous also according to the ISO 13528 standard.

$$99 \quad s_s \leq 0.3\sigma_{pt} \quad (1)$$

100 Where

101  $s_s$ = between-sample standard deviation

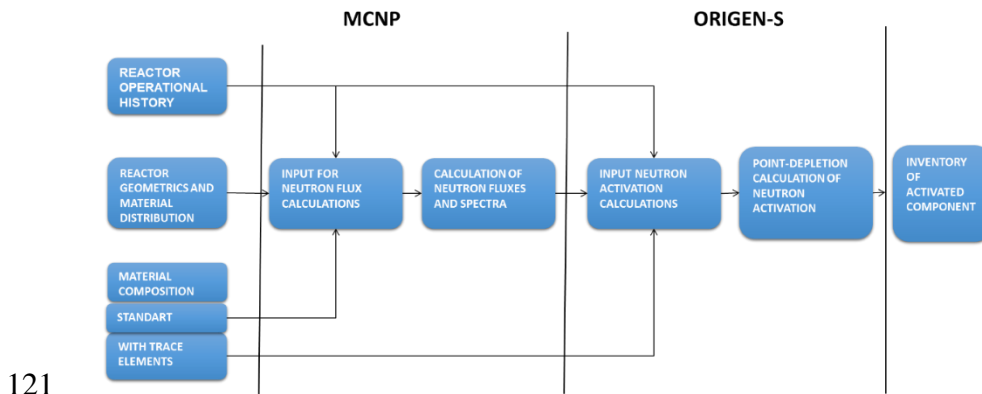
102  $\sigma_{pt}$ = robust standard deviation of participant results

103 The stability of the samples was considered in theoretical level based on the experience of  
 104 the participants. The sample preparation, transport and storage were considered not to  
 105 affect the stability of the samples, as they were solid materials and the DTMs were not  
 106 volatile in normal storage and transport conditions. The only exception was  $^3\text{H}$ , which can  
 107 be lost due to evaporation as tritiated water even at room temperature. Loss of  $^3\text{H}$  is  
 108 especially problematic if it originates from contamination. In this study,  $^3\text{H}$  originated from

109 activation and all loosely bound  $^3\text{H}$  was considered to have been released already during  
 110 sampling. Evidence for  $^3\text{H}$  instability would have been possible to be carried out by  
 111 comparing the submitted results with the measurement dates [3].

## 112       **Activation calculations**

113 Estimating the activation reactions in the reactor structures was a two-stage process. First,  
 114 a particle transport code was used to solve the neutron fluxes inside the reactor structures  
 115 and components and then this data was used in a point-depletion code, which took the  
 116 energy dependent neutron flux values from the transport calculations together with the  
 117 material composition data and operating history to determine the quantity of neutron  
 118 activation products. This study applied Monte Carlo based neutron transport code MCNP  
 119 [10] and a point-depletion code ORIGEN-S [6]. The procedure utilised is presented in Fig.  
 120 1 [11].



121  
 122 **Fig. 1** Overview of the applied calculation steps [11]

123 The activation calculations modelled the whole operating history of the FiR1 research  
 124 reactor throughout the years 1962-2015 as described in Ref. [11]. Major structural changes  
 125 during the reactor operating history were taken into account by creating different neutron  
 126 transport models for different phases of the operating history and combining all of these in  
 127 the point-kinetic calculation. Altogether three separate time periods were modelled.

128 The biological shield concrete core was drilled close to a horizontal neutron beam tube.  
 129 The beam tube had been plugged in the late 1980's. However, it was impossible to model  
 130 the details of all the experiments and research devices used inside the beam tube in the  
 131 1960's and 1970's. Therefore, the calculation model assumed conservatively that the beam  
 132 tube had been empty before the plugging, whereas in reality, several different types of  
 133 research equipment with unknown time intervals had been placed inside the beam ports  
 134 causing unknown amounts of neutron absorption and scattering. This assumption  
 135 overestimated the neutron fluxes around the beam tube, but was considered acceptable for  
 136 conservative initial calculations in estimation of total waste volumes. The calculation  
 137 results were used in this article by assuming that the concrete nuclide vector (relative  
 138 nuclide-wise activities) was correct and the results were scaled using the measured gamma-  
 139 activities from the key nuclide  $^{152}\text{Eu}$ .

140 Although the neutron flux was estimated conservatively, the chemical composition of the  
 141 concrete used in the calculation model was determined from three inactive cores that had  
 142 been drilled earlier from the inactive outer parts of the reactor structure as described earlier  
 143 [7]. The samples were homogenised and their compositions were measured separately  
 144 using CHN pyrolyser (C, H and N), AOX pyrolyser (Cl), ICP-MS (B, Ba, Co, Cs, Eu, Li,  
 145 Ni, Sm and U), and ICP-OES techniques (Al, Ca, Fe, K, Mg, Mn, P, S, Si and Ti). For  
 146 conservatism, the highest measured concentration (or LOD) of each activating element was  
 147 used in the calculation model. The concentration results of the relevant stable elements for  
 148 this study in the three core samples are shown in Table 1. Point-depletion code ORIGEN-  
 149 S uses built-in ENDF/B-VI formatted cross sections, but for illustration, Table 1 also lists  
 150 the activation reactions and reaction cross sections according to Ref. [12].

151 **Table 1** Concentrations of elements of interest in three inactive concrete subsamples  
 152 (internal data), activation reactions and thermal activation cross sections

Element	Concentrations of three inactive concrete subsamples (mg kg <sup>-1</sup> )	Activation reaction	Reaction thermal neutron cross section (barns)
Li	36/27/39	$^6\text{Li}(n,\alpha)^3\text{H}$	936±6
C	1730/1835/2165	$^{13}\text{C}(n,\gamma)^{14}\text{C}$	$(0.9 \pm 0.05) \times 10^{-3}$
N	<200	$^{14}\text{N}(n,p)^{14}\text{C}$	1.75±0.05

Cl	55/56/59	$^{35}\text{Cl}(n, \gamma)^{36}\text{Cl}$	90±30
Ca	91000/79000/95000	$^{40}\text{Ca}(n, \gamma)^{41}\text{Ca}$	0.22±0.04
Fe	23000/21000/23000	$^{54}\text{Fe}(n, \gamma)^{55}\text{Fe}$	2.7±0.4
Ni	<50	$^{62}\text{Ni}(n, \gamma)^{63}\text{Ni}$	15±2
Eu	2.1/2.0/2.2	$^{151}\text{Eu}(n, \gamma)^{152}\text{Eu}$	5500±1500
		$^{153}\text{Eu}(n, \gamma)^{154}\text{Eu}$	1500±400
Co	12/13/13	$^{59}\text{Co}(n, \gamma)^{60}\text{Co}$	20.2±1.9

### 153 **Methodology for statistical analysis**

154 Statistical analysis of the submitted results was carried out using the ISO 13528 standard  
 155 on proficiency testing by interlaboratory comparison [3]. One major drawback of the ISO  
 156 13528 standard is the lack of uncertainty considerations of the submitted results. However,  
 157 due to consistency, the ISO 13528 standard was utilised similar to the first year [2]. As the  
 158 studied activated concrete was not a reference material, the assigned values were calculated  
 159 using the submitted results. Robust means and robust standard deviations were calculated  
 160 using Algorithm A, which is robust for outliers. The iterations of the robust mean and  
 161 standard deviations were continued until there was no change in their third significant  
 162 figure [3]. The robust means and standard deviations calculated from the participant's  
 163 results are referred to as measured assigned values. The submitted results were also  
 164 compared with calculated assigned values, which were determined based on the activation  
 165 reactions.

166 Performance assessment was carried out using z score of Eq. (2), which was a  
 167 recommended method in cases when the assigned value is calculated from the submitted  
 168 results [3]. The submitted results (noted  $x_i$ ) were assessed against both measured assigned  
 169 values and calculated assigned values. In cases, when the robust standard deviation was  
 170 large e.g. over 20%, the uncertainty of the assigned value  $u(x_{pt})$  calculated using Eq. (3)  
 171 was used as  $\sigma_{pt}$  [3]. Selection of the  $u(x_{pt})$  as  $\sigma_{pt}$  was the prerogative of the intercomparison  
 172 exercise organiser in order to produce fit for purpose assessments [3]. The z score results



173 were acceptable when  $|z| \leq 2.0$ , a warning signal was given for results with  $2.0 < |z| <$   
174  $3.0$ , and  $|z| \geq 3.0$  results were unacceptable [3].

175

$$176 \quad z_i = (x_i - x_{pt}) / \sigma_{pt} \quad (2)$$

177

178 where

179  $x_i$  = the value given by a participant  $i$

180  $x_{pt}$  = the assigned value

181  $\sigma_{pt}$  = standard deviation for the proficiency assessment

$$182 \quad u(x_{pt}) = 1.25 \times s^* / p^{0.5} \quad (3)$$

183 where

184  $s^*$  = robust standard deviation of the results

185  $p$  = number of samples

## 186 **Overview of the radiochemical analyses**

187 The radiochemical methods utilised in the DTM analysis of the activated concrete have  
188 been summarised by Leskinen et al. [4]. The utilised procedures were mainly based on  
189 published references [13-27], but also internal procedures and modifications based on  
190 discussions between the participating laboratories. The main focus was given for  $^3\text{H}$ ,  $^{14}\text{C}$ ,  
191  $^{55}\text{Fe}$  and  $^{63}\text{Ni}$  whereas  $^{36}\text{Cl}$  and  $^{41}\text{Ca}$  were optional. In general, the applied methods were  
192 divided between the volatile (e.g.  $^3\text{H}$ ,  $^{14}\text{C}$  and  $^{36}\text{Cl}$ ) and non-volatile (e.g.  $^{41}\text{Ca}$ ,  $^{55}\text{Fe}$  and  
193  $^{63}\text{Ni}$ ) DTMs. The volatile DTMs were mainly analysed using thermal oxidation using a  
194 Pyrolyser (RADDEC) or an Oxidiser (Perkin Elmer) system. In thermal oxidation systems,  
195 volatile DTMs were trapped in different trapping solutions e.g.  $^3\text{H}$  in 0.1 M  $\text{HNO}_3$  solution,  
196  $^{14}\text{C}$  in CarboSorb or CarbonTrap solutions, and  $^{36}\text{Cl}$  in 6 mM  $\text{Na}_2\text{CO}_3$  solution. The  $^3\text{H}$  and  
197  $^{14}\text{C}$  solutions were directly analysed in the trapping solutions using Liquid Scintillation  
198 Counting (LSC) whereas  $^{36}\text{Cl}$  solutions required further purifications using  $\text{AgCl}$

199 precipitation and anion exchange resin prior to the LSC measurements. One laboratory also  
200 carried out the  $^{14}\text{C}$  and  $^{36}\text{Cl}$  analysis using a closed system on a heating mantle.

201 Even though the solubility of activated concrete was a major challenge and alkali fusion  
202 may have been a better method of choice, all the participants utilised acid digestion method  
203 for the destruction of the solid matrix in the analysis of non-volatile DTMs. Both acid  
204 digestions on heating mantles, hotplates and microwave ovens were utilised with strong  
205 acids i.e. mixtures of HCl, HNO<sub>3</sub>, HF, HClO<sub>4</sub>. The successfulness of acid digestions is  
206 discussed in the results section. After the acid digestions, mainly hydroxide precipitations  
207 with NaOH or NH<sub>4</sub>OH were implemented in order to separate Fe and Ni from Cs, Sr, Ba,  
208 Ra and namely Ca, if analysed. This precipitation was recommended during project  
209 discussion to be carried out very carefully with saturated NaOH up to pH 1 and then with  
210 mild NaOH (<0.5 M) to pH 8-9. Use of mild NaOH was proposed to prohibit precipitation  
211 of Ca in lower pH range resulting either in lower Ca yields in Ca fraction or Ca interference  
212 in Fe and Ni separations. Fe and Ni were separated from each other and from cobalt using  
213 an anion exchange resin. However, one laboratory precipitated and removed AgCl prior to  
214 Fe and Ni separation using TRU resin and another laboratory carried out anion exchange  
215 resin separation of Fe and Ni without hydroxide precipitation. Purified Fe fractions were  
216 evaporated to dryness and the residue was dissolved into 0.5M HNO<sub>3</sub> or 1M/3M H<sub>3</sub>PO<sub>4</sub>,  
217 the latter acid has been discussed to cause the least amount of color quenching in LSC  
218 measurements [2,27]. Ni fractions after the anion exchange resin treatment were further  
219 purified with Ni resin (Eichrom Technologies) once or twice. The purified Ni fractions  
220 were evaporated to lower volumes prior to LSC measurements.

221 Two laboratories based their analyses of  $^{41}\text{Ca}$  on sequential precipitations of Ca as  
222 carbonates and hydroxides. Precipitations were carried out with and without heating and  
223 the precipitates and supernatants were separated using centrifugations. Contrary to  
224 referenced procedures in which the final hydroxide precipitate was dissolved in 4 M HCl  
225 and pH of the solution raised to pH 6-7 [19] or dissolved in 0.1 M HCl [17], the precipitate  
226 was recommended to be dissolved into conc. HCl and evaporated to dryness in order to  
227 produce water soluble CaCl<sub>2</sub>. The CaCl<sub>2</sub> precipitate was dissolved in small amount of  
228 deionised water (3-4 ml) prior to the LSC measurements.

229 One laboratory purified Ca-containing solution, separated from Fe and Ni by their  
230 hydroxide precipitation, with oxalate precipitation of Ca from the solution and two  
231 different anion exchange steps. Ca oxalate precipitation was calcined at 600 °C over night  
232 and dissolved to 8 M HCl prior to first anion exchange separation. Ca was eluted in 8 M  
233 HCl, evaporated and dissolved to 8 M HNO<sub>3</sub> for the second anion exchange separation. Ca  
234 was eluted in 8 M HNO<sub>3</sub> and the acid fraction was evaporated to dryness. The residue was  
235 dissolved in 3-4 ml of 0.1 M HCl and measurements of stable Ca by MP-AES (Microwave  
236 Plasma - Atomic Emission Spectrometer) and <sup>41</sup>Ca by LSC were followed.

237 The LSC measurements of all DTMs (i.e. volatile and non-volatile) were carried out by  
238 mixing aliquots of the purified fractions with liquid scintillation cocktails (mainly Ultima  
239 Gold, but also Optiphase HiSafe 3) prior to the LSC measurements using counters such as  
240 Quantulus 1220 LSC, HIDEX 300SL, and AccuFLEX LSC-8000. The measurement  
241 efficiencies were determined using standard solutions for quenching corrections or TDCR  
242 (Triple-to-Double Coincidence Ratio) technique [28].

243 The <sup>3</sup>H and <sup>14</sup>C yields were determined using experimental estimations based on behaviour  
244 of liquid standards. <sup>36</sup>Cl, <sup>41</sup>Ca, <sup>55</sup>Fe and <sup>63</sup>Ni yields were determined using UV-Vis, ICP-  
245 OES, ICP-MS, MP-AES or standard addition. In one case, Fe yield was estimated to be  
246 90% based on the in-house experience. The yields are further discussed in results section  
247 as the solubility of the matrix was not always complete and the concrete contained  
248 significant amounts of stable Fe, which was not always diligently considered in yield  
249 corrections.

## 250 **Overview of the gamma spectrometric analyses**

251 All the laboratories carried out analysis of <sup>152</sup>Eu and <sup>60</sup>Co in solid form. Some laboratories  
252 also carried out gamma analysis of dissolved samples but the results suffered from low  
253 activities due to low sample sizes. The geometries of the solid sample measurements were  
254 glass/plastic vials and a petri dish. The samples were placed on top of high purity  
255 Germanium (HPGe) detectors, which all participants utilised. Variety of efficiency  
256 calibrations were used, namely calibration solutions with LVis (Gamma vision) with

257 EFFTRAN coincidence correction, ISOCS or LabSOCS (Mirion Technologies) and dual  
258 polynomial fitting. One laboratory carried out efficiency corrections based on experience  
259 due to lack of efficiency calibration for the LSC vial geometry. One laboratory prepared  
260 in-house concretes spiked with gamma emitters to establish an efficiency calibration  
261 specific for concretes.

## 262 **DTM and gamma emitter results and statistical analysis**

263 The complete destruction of the solid matrix was challenged by the low solubility of  
264 concrete even in strong acids. Even though majority of the laboratories reported up to 100%  
265 dissolution with exception of proposed silica residues, in some cases the completeness of  
266 the acid digestions was estimated to be as low as 60% (Table 2). Additionally, it was not  
267 completely clear how some laboratories took into consideration the original amounts of  
268 Ca, Fe and Ni in the activated concrete, because only three laboratories carried out the  
269 chemical composition analysis of the acid digested solutions. Especially large amount of  
270 Fe caused significant problems in the ion exchange resin separations and result calculations  
271 as discussed later. Large amount of stable Ca did not affect the results as much as Fe, since  
272 Ca was analysed only by a couple of laboratories and majority of them analysed its content  
273 in the acid digested solution. Stable Ni content was low compared to the amount of added  
274 Ni carrier (0.05 to 4 mg) and therefore, its original content did not affect the results.  
275 Comparison of Table 1 and 2 show that on average, the participant's Ca concentration  
276 results were 58-81% of the concentrations used in the activation calculations, Fe results  
277 were 82-95% whereas Ni results were below or close to detection limit and therefore not  
278 applicable. One reason for the difference may be, that the dissolution of Fe and larger  
279 fraction of Ca has not been complete with the selected methods of three reported  
280 laboratories. Additionally, the data in Table 1 was measured from another FiR1 core  
281 sample, which was on a different height of the biological shield, which may have contained  
282 different types of stones. However, it is unfortunate that elemental concentration data is  
283 not available from all participating laboratories, especially from the ones that reported  
284 complete dissolution of the concrete material.

285 **Table 2** Stable Ca, Fe and Ni concentrations in the activated concrete based on acid  
 286 digestion results

ID #	Estimated completeness of acid digestion (%)	Ca (mg/g) $\pm 2\sigma$	Fe (mg/g) $\pm 2\sigma$	Ni (mg/g) $\pm 2\sigma$
1	100	-	-	-
2	<100, silica residue	-	-	-
3	100	-	-	-
4	85	51 $\pm$ 10	21 $\pm$ 4*	0.020 $\pm$ 0.006
5	-	-	-	-
6	100, silica residue	71 $\pm$ 10	19 $\pm$ 3	<LOD
7	60	54 $\pm$ 8	18 $\pm$ 2	<LOD
8	100, silica residue	-	-	-

287 \*estimated from Ni yield during the leaching step (the loss of stable Fe for the leaching  
 288 step was assumed to be the same as for stable Ni carrier, i.e. 70 %)

289 In total, 13 <sup>55</sup>Fe and <sup>63</sup>Ni results were submitted and the entries with sample numbers,  
 290 sample sizes, yields and activity concentrations are presented in Table 3. The results show  
 291 that 7 out of 13 <sup>55</sup>Fe entries were above limit of detection (LOD) and minimum amount of  
 292 sample to produce activity concentration results above LOD was 3 g. However, the results  
 293 varied significantly from 0.1 to 8.1 Bq g<sup>-1</sup>. The large variation was estimated to originate  
 294 from a combination of the following parameters i) varying completeness of the acid  
 295 digestions affecting the activity concentration calculations, ii) the high original stable Fe  
 296 content, which was not always analysed or taken into consideration, iii) possible  
 297 interference caused by luminescence, quenching and spectral interferences, and iv) low  
 298 activity. Since the <sup>55</sup>Fe activity concentration results varied significantly, the statistical  
 299 analysis was not possible. Additionally, the yields for <sup>55</sup>Fe varied significantly from 13%  
 300 to 101%. However, not enough information on the yield calculations (i.e. how original Fe  
 301 in the concrete was considered) was submitted.

302 <sup>63</sup>Ni results in Table 3 show that only 3 out of 13 results were above LOD and minimum  
 303 amount of sample to produce measurable activity concentrations was 5 g. The purified <sup>63</sup>Ni

304 fraction of sample number 7 with 10 g of concrete suffered from burning of DMG  
 305 precipitate causing significant colour quenching. Even though 3 entries were not  
 306 considered to be a sufficient amount of data entries for reliable statistical analysis, 10  
 307 iterations with Algorithm A were carried out in order to produce fit for purpose  $^{63}\text{Ni}$   
 308 assigned value, namely  $970 \pm 380 \text{ mBq g}^{-1}$  ( $2\sigma$ ). As the robust standard deviation of the  
 309 assigned value was above 20% (i.e. 27%), standard uncertainty of the assigned value was  
 310 utilised in the z score calculations. As such, all the  $^{63}\text{Ni}$  data entries above LOD were in  
 311 acceptable z score range. On the other hand, some of the submitted LOD values are  
 312 significantly below the assigned value, especially for samples 1 and 8. Critical  
 313 considerations in LOD calculations are discussed later whereas here the results show  
 314 clearly that LOD calculations need to be carried out carefully. The yield for  $^{63}\text{Ni}$  was 24-  
 315 114%, varying similarly with the corresponding values for  $^{55}\text{Fe}$ . One participant, which did  
 316 not carry out Ca analysis (i.e. no separation of Ca from Ni and Fe) reported difficulties in  
 317 Ni purifications with Ni resin due to precipitation of Ca causing lowered yield of sample 4  
 318 [15]. Additionally, one laboratory reported Ni yields above 100%, which were considered  
 319 acceptable due to approximately 30% uncertainty ( $2\sigma$ ).

320 **Table 3** Measured  $^{55}\text{Fe}$  and  $^{63}\text{Ni}$  activity concentrations and corresponding masses, yields  
 321 and z-scores compared to measured assigned value, if applicable

ID #	Mass (g)	$^{55}\text{Fe}$ results		$^{63}\text{Ni}$ results		
		Yield (%)	Activity concentration ( $\text{mBq g}^{-1}$ )	Yield (%)	Activity concentration ( $\text{mBq g}^{-1}$ )	z-score meas.
1	3	90	$370 \pm 20$	24	<100	
1	3	95	$340 \pm 20$	83	<100	
1	3.5	101	$350 \pm 20$	90	<100	
2	10	64	$1590 \pm 940$	24	$700 \pm 160$	1.4
3	5	90*	$8100 \pm 200$	99	$1100 \pm 200$	0.7
4	5	58***	<340	30	<310	
5	10	**	$110 \pm 40$	**	$1120 \pm 150$	0.8
6	0.6	13	<500	114	<600	
6	0.6	18	<400	102	<600	
6	0.6	19	<400	101	<600	
7	10	57	$2600 \pm 4100$	77	<450	
8	0.5	32	<500	87	<90	
8	0.5	53	<300	85	<90	

322 \*estimated, \*\*data not submitted, \*\*\*the loss of stable Fe for the leaching step was  
323 assumed to be the same as for stable Ni carrier (around 70 %)

324 In total, 5  $^3\text{H}$  and  $^{14}\text{C}$  results were submitted and the entries with sample numbers, sample  
325 sizes, yields and activity concentrations are presented in Table 4. All the  $^3\text{H}$  activity  
326 concentration results were above LOD and the statistical analysis was carried out by 2  
327 iterations resulting in the  $^3\text{H}$  assigned value of  $55\pm 4 \text{ Bq g}^{-1}$  ( $2\sigma$ ). As the robust standard  
328 deviation was low (i.e. 6%), it was used in the z score calculations, which show that all the  
329 results were in acceptable range. The presented yields were also good corresponding to  
330 efficient extraction of  $^3\text{H}$  using thermal oxidation.

331 The  $^{14}\text{C}$  results in Table 4 show that only one result out of 5 data entries was above LOD  
332 and it was produced using traditional oxidative acid digestion in a closed heating mantle  
333 system. A discrepancy can be observed between samples 5 and 6 as 10 times higher amount  
334 of sample produced lower LOD than the only activity concentration result above LOD. The  
335 efficient extraction of  $^{14}\text{C}$  using thermal oxidation is also shown in the  $^{14}\text{C}$  results as in the  
336  $^3\text{H}$  results. However, the challenges and other critical considerations are discussed later.

337 **Table 4** Measured  $^3\text{H}$  and  $^{14}\text{C}$  activity concentrations and corresponding masses, yields  
338 and z-scores compared to measured assigned values, if applicable

ID #	Mass (g)	$^3\text{H}$ results			$^{14}\text{C}$ results	
		Yield (%)	Activity concentration ( $\text{Bq g}^{-1}$ )	z-score meas.	Yield (%)	Activity concentration ( $\text{mBq g}^{-1}$ )
5	0.5	*	$51\pm 14$	1.2	*	$70 \pm 10$
6	5	90	$53\pm 11$	0.7	100	< 40
6	1	90	$56\pm 11$	0.3	100	< 200
8	1	76	$58\pm 13$	0.8	100	< 2500
8	1	76	$58\pm 13$	0.8	100	< 2500

339 \*data not submitted

340 The analyses of  $^{36}\text{Cl}$  and  $^{41}\text{Ca}$  were optional. The submitted results are summarised in Table  
341 5 and they show that only one result is above LOD, namely  $6\pm 1 \text{ mBq g}^{-1}$ .  $^{36}\text{Cl}$  analysis was  
342 carried out by two laboratories and the results show that sample 8 suffered from severe loss

343 of Cl carried (i.e. 5% yield) whereas 10 g of sample 5 with high yield (93-98%) was able  
344 to produce activity concentration results above LOD.

345 Even though several analyses were carried out in order to submit  $^{41}\text{Ca}$  results (Table 5), all  
346 laboratories reported difficulties in the LSC measurement either due to spectral interference  
347 (sample 5), or significant quenching with white colour (samples 6-7). The spectral  
348 interference was based on an observation of an unknown signal in the LSC spectrum and  
349 it was initially hypothesised to originate from  $^{45}\text{Ca}$ . However, assessment of the  $^{45}\text{Ca}$  half-  
350 life (i.e. 163 days) and cooling time (i.e. 5 years) out ruled the hypothesis and the cause of  
351 the interference remained unknown. The colour quenching and other critical considerations  
352 in  $^{41}\text{Ca}$  analysis are discussed in later section. The yield for  $^{41}\text{Ca}$  was 24-93%, varying  
353 widely as with other determined radionuclides.

354 **Table 5** Measured  $^{36}\text{Cl}$  and  $^{41}\text{Ca}$  activity concentrations and corresponding masses and  
355 yields

ID #	Mass (g)	$^{36}\text{Cl}$ results		$^{41}\text{Ca}$ results	
		Yield (%)	Activity concentration ( $\text{mBq g}^{-1}$ )	Yield (%)	Activity concentration ( $\text{mBq g}^{-1}$ )
5	10	93-98	$6 \pm 1$	>93	Spectral interference
6	0.6	-	-	34	<300
6	0.6	-	-	24	<400
6	0.6	-	-	24	<400
6	1.8	-	-	33	<70
7	10	-	-	68	<500
8	2	5	<400	-	-

356 The main gamma emitters, namely  $^{152}\text{Eu}$  and  $^{60}\text{Co}$ , were optional and the results are  
357 summarised in Table 6. The efficiency calibration for sample 3 was based on experience  
358 whereas other results were calibrated as discussed earlier. The  $^{152}\text{Eu}$  assigned value was  
359 iterated 10 times to be  $21 \pm 2 \text{ Bq g}^{-1}$  ( $2\sigma$ ). As the robust standard deviation of the assigned  
360 value was low (i.e. 8%), it was used in the z score calculations. The results show that only  
361 one  $^{152}\text{Eu}$  entry was in unacceptable range ( $z \geq 3$ ) whereas all the other entries were in  
362 acceptable range ( $z \leq 2$ ).



363 The  $^{60}\text{Co}$  assigned value  $280 \pm 60$  mBq/g ( $2\sigma$ ) was iterated 8 times from 7 data entries. As  
 364 the robust standard deviation of the assigned value was above 20% (i.e. 24%), the  
 365 uncertainty of assigned value was utilised in the z score calculations. The  $^{60}\text{Co}$  z score  
 366 results show that three results were in warning signal range and all the others in acceptable  
 367 range.

368 **Table 6** Measured  $^{152}\text{Eu}$  and  $^{60}\text{Co}$  activity concentrations and corresponding masses,  
 369 yields and z-scores compared to measured assigned value  
 370

ID #	Mass (g)	$^{152}\text{Eu}$ results		$^{60}\text{Co}$ results	
		Activity concentration ( $\text{Bq g}^{-1}$ )	z-score meas.	Activity concentration ( $\text{mBq g}^{-1}$ )	z-score meas.
1	20	$21 \pm 2$	0.4	$360 \pm 30$	2.5
2	2	$26 \pm 0.3$	3.4	$360 \pm 110$	2.5
3	20	$19 \pm 1$	1.0	$220 \pm 40$	1.9
4	16	$22 \pm 4$	0.7	$260 \pm 50$	0.6
5	12	$19 \pm 2$	1.1	$202 \pm 20$	2.5
6	20	$20 \pm 0.2$	0.2	$260 \pm 10$	0.6
7	18	$20 \pm 0.3$	0.4	$250 \pm 20$	1.0
8	20	$21 \pm 2$	0.2	$270 \pm 30$	0.3

371

## 372 **Activation calculation results**

373 Table 7 lists the specific activities of the activated concrete samples, which had been  
 374 calculated previously using conservative assumptions on the beam tube operation [5]. As  
 375 the homogeneity measurements for  $^{152}\text{Eu}$  showed, the measured activity concentration of  
 376  $20 \text{ Bq g}^{-1}$  was significantly lower than corresponding calculated  $^{152}\text{Eu}$  activity  
 377 concentration i.e.  $480 \text{ Bq g}^{-1}$ . However, nuclear waste management procedures typically  
 378 use non-destructive methods (i.e. calculations in the first place) to estimate total waste  
 379 volumes with conservative assumptions and eventually the waste is classified using  
 380 validated nuclide vectors and measured key nuclide activity concentration. The same  
 381 procedure was utilised here by scaling the calculated DTMs with measurement based  
 382 assigned value of  $^{152}\text{Eu}$  (i.e.  $21 \pm 2 \text{ Bq g}^{-1}$ ), which was iterated from the participants' results  
 383 (see Table 6 and corresponding text). This means a scaling factor of  $21/480 = 0.0438$ .

384 Another possibility would have been to choose  $^{60}\text{Co}$  as the key nuclide. In the second case,  
 385 the scaling factor would have been 0.028, which had resulted in 36 percent difference in  
 386 the final results. This indicates that there was some difference between the Co and Eu  
 387 concentrations in the studied samples compared to the samples that were used to determine  
 388 the original composition used in the calculation system. However, this is still minor  
 389 compared to the uncertainties in the original assumptions of the neutron dose to the  
 390 samples.

391 Additionally, the results in Table 7 show that the calculated activity concentrations  
 392 decrease in order  $^3\text{H} \gg ^{152}\text{Eu} > ^{41}\text{Ca} > ^{14}\text{C} > ^{60}\text{Co} > ^{63}\text{Ni} > ^{55}\text{Fe} > ^{36}\text{Cl}$  even though the  
 393 chemical composition of the activating elements (Table 1) decrease in order  $\text{Ca} > \text{Fe} \gg \text{C}$   
 394  $> \text{N} > \text{Cl} > \text{Ni} > \text{Li} > \text{Co} > \text{Eu}$  exhibiting significance of the thermal cross sections.

395 The  $2\sigma$  uncertainties presented with the calculated activity concentrations were calculated  
 396 using law of error propagation in multiplication. In principle, the sources of uncertainties  
 397 are mass, irradiation time, reaction cross sections and neutron flux. The highest uncertainty  
 398 derives from the sample composition, i.e. masses of the activating impurities. The FiR1  
 399 biological shield concrete is heterogeneous and there can be a large variation between the  
 400 ratio of rocks and cement in different cores. The calculations used the measured  
 401 composition, but since the studied sample was from another drill core, it may have  
 402 contained slightly different rock and cement ratio and therefore an uncertainty of twenty  
 403 percent was assumed. As the irradiation and decay time is based on operating diaries and  
 404 therefore very well-known, an uncertainty of one month was assumed. Cross section  
 405 uncertainties were estimated according to the values listed in Table 1 [29]. Due to the  
 406 assumption in the reactor beam tube operations, neutron flux uncertainty is taken into  
 407 account by comparing only the results correlated with measured assigned activity of  $^{152}\text{Eu}$ .

408 **Table 7**  $^3\text{H}$ ,  $^{14}\text{C}$ ,  $^{36}\text{Cl}$ ,  $^{41}\text{Ca}$ ,  $^{55}\text{Fe}$ ,  $^{63}\text{Ni}$ ,  $^{152}\text{Eu}$  and  $^{60}\text{Co}$  activation calculation results with  $2\sigma$   
 409 uncertainty

Radionuclide	Conservative calculated activity concentration with $2\sigma$ uncertainty (mBq g <sup>-1</sup> )	Calculated activity concentration with $2\sigma$ uncertainty (mBq g <sup>-1</sup> )

		<b>correlated with measured assigned value of <math>^{152}\text{Eu}</math></b>
$^3\text{H}$	4500000±900000	200000±40000
$^{14}\text{C}$	12000±4400	530±190
$^{36}\text{Cl}$	530±210	23±9
$^{41}\text{Ca}$	21000±5600	890±240
$^{55}\text{Fe}$	1600±400	66±17
$^{63}\text{Ni}$	7600±1800	340±80
$^{152}\text{Eu}$	480000±160000	21000±7200
$^{60}\text{Co}$	10000±2100	430±90

410 \*measured assigned value derived from participants' results

411 Comparison of the measured DTM and gamma emitter results with the  $^{152}\text{Eu}$  corrected  
412 calculated results in Table 7 shows varying degrees of correlation. The best correlations  
413 can be seen between the  $^{152}\text{Eu}$  corrected  $^{60}\text{Co}$  calculated result ( $430\pm90\text{ mBq g}^{-1}$ ) and the  
414 measured  $^{60}\text{Co}$  assigned value ( $280\pm60\text{ mBq g}^{-1}$ ) which is 65% of the calculated result. The  
415 second best correlation can be seen with the measured  $^3\text{H}$  assigned value ( $55\pm4\text{ Bq g}^{-1}$ ),  
416  $^{14}\text{C}$  (one result,  $70\pm10\text{ mBq g}^{-1}$ ) and  $^{36}\text{Cl}$  (one result,  $6\pm1\text{ mBq g}^{-1}$ ) results with the  
417 corresponding  $^{152}\text{Eu}$  corrected calculated results which are approximately 28%, 13%, and  
418 26% of the calculated values ( $200\pm40\text{ Bq g}^{-1}$ ,  $530\pm190\text{ mBq g}^{-1}$ ,  $23\pm9\text{ mBq g}^{-1}$ ,  
419 respectively). The measured  $^3\text{H}$ ,  $^{14}\text{C}$  and  $^{36}\text{Cl}$  results are systematically below the  
420 calculated results. The  $^3\text{H}$  results may have been affected by diffusion of HTO within the  
421 biological shield, isotopic exchange with the atmospheric hydrogen or evaporation during  
422 sample preparation [30,31]. Therefore, the correlation can be considered satisfactory. Also  
423 the  $^{36}\text{Cl}$  and  $^{14}\text{C}$  values can be considered satisfactory given the difficulties in measurement  
424 of stable Cl, N and C for the activation calculations of  $^{36}\text{Cl}$  and  $^{14}\text{C}$  at such low activities.  
425 Additionally, the chemical composition of the main element to produce  $^{14}\text{C}$ , namely N, has

426 been given in the Table 1 as below  $200 \text{ mg kg}^{-1}$  giving a conservative result in the activation  
427 calculations. As such analyses of Cl, N and C are not easy in concrete and the activation  
428 calculations may suffer from many uncertainties (see section “Activation calculation  
429 results”), which can explain the observed differences between calculated and measured.

430 Significant differences can be seen between the calculated and the measured  $^{55}\text{Fe}$  results.  
431  $^{55}\text{Fe}$  results were from almost twice to over hundred times above the calculated value. The  
432 chemical analysis of stable Fe is quite straightforward process using ICP-OES as long as  
433 the element has been quantitatively released from the solid matrix. Therefore, the main  
434 reason for the deviating measured results from calculated may be the uncorrect yield  
435 correction in the measurement results as discussed before. Additionally, the  $^{55}\text{Fe}$  results in  
436 the activated steel [2] were also significantly different to the calculated results and one of  
437 the reasons for deviation was proposed to be the short half life (2.7 years) and unknown  
438 cooling time.

439 The measured  $^{63}\text{Ni}$  assigned value (i.e.  $970 \pm 380 \text{ mBq g}^{-1}$ ) is almost three times higher than  
440 the calculated result (i.e.  $340 \pm 80 \text{ mBq g}^{-1}$ ). This is surprising as the original Ni content in  
441 Table 1 was indicated to be below  $50 \text{ mg kg}^{-1}$  and therefore, the calculated result was  
442 expected to be an overestimation rather than underestimation compared to the measured  
443  $^{63}\text{Ni}$  content. One possible reason for this could be presence of interfering radionuclides,  
444 such as  $^{60}\text{Co}$  and  $^{55}\text{Fe}$ , in the  $^{63}\text{Ni}$  fraction. Even though no participant reported difficulties  
445 with interfering radionuclides, it is still possible that their presence has been unknown,  
446 undetermined or underestimated. Other assumptions can be linked to the presence of  
447 calcium or quenching effects in LSC due to concrete matrix which can bias the  
448 measurement of  $^{63}\text{Ni}$  content. Yet another possibility, which has been acknowledged  
449 earlier, is that the original stable Ni compositions in the activated and inactive concrete  
450 samples were different.

#### 451 *Considerations in the activation calculations*

452 Concrete is especially difficult material, since it is very inhomogeneous and even small  
453 variations in the ratio between rocks and cement can have a large effect if some activating

454 impurity is mainly present in either one them. However, activity calculations provide a  
455 non-destructive first approach to estimate the volumes and activities in a decommissioning  
456 project. Especially research reactors typically have very complicated operating history,  
457 which may also contain several structural modifications. Therefore, the calculations at the  
458 FiR1 research reactor decommissioning project also required several simplifying  
459 assumptions. These were always chosen conservatively to slightly overestimate the amount  
460 of activated waste. The assumptions on the operating history of the horizontal neutron  
461 beam tubes appeared to be slightly over conservative, which caused the large discrepancy  
462 between the calculated and measured activities. However, dismantling planning also  
463 contain other factors (e.g. mechanical and logistics) that may affect choosing the final  
464 cutting and waste management methods. Therefore, optimising the calculations for high-  
465 precision validation purposes can be very complicated.

#### 466 *Critical considerations in the DTM analysis*

467 The first critical step in the analysis of non-volatile DTMs is the quantitative release of the  
468 analytes of interest from the solid matrix. Solubility of RPV steel was not problematic as  
469 seen in the results of the first intercomparison exercise [1,2], whereas activated concrete  
470 required harsh acid digestion treatments in order to obtain complete destruction of the solid  
471 matrix. Measurement of the chemical composition of the acid digested solution is critical  
472 for appropriate addition of carriers and subsequently yield correction and also for the  
473 determination of possible interfering stable elements (e.g. Ca and Co in Ni resin  
474 separations).

475 Critical considerations of  $^{14}\text{C}$ ,  $^{55}\text{Fe}$  and  $^{63}\text{Ni}$  analysis were discussed by Leskinen et al. [2].  
476 As a summary, reliable  $^{14}\text{C}$  analysis requires quantitative release and conversion of carbon  
477 to  $\text{CO}_2$  and trapping it into a trapping solution. In the case of acid digestion, oxidative acids  
478 are required and in the case of thermal oxidation, a catalyst and oxygen gas are needed in  
479 the  $\text{CO}_2$  conversion. In thermal oxidation, the release of the analyte is also affected by  
480 temperature, which needs to follow appropriate profile based on the matrix. In addition,  
481 the yield of  $^{14}\text{C}$  analysis is determined by spiking with liquid  $^{14}\text{C}$  standards, as there are no

482 commercially available reference materials. These discussions are relevant also for the  $^{14}\text{C}$   
483 analysis in activated concrete. However, due to low  $^{14}\text{C}$  activity concentration of the  
484 studied activated concrete, almost all results were below LOD. Therefore, further studies  
485 with higher  $^{14}\text{C}$  activity level activated concrete should be conducted. As developed in Ref.  
486 [32], the preparation of spiked in-house concretes should be investigated to determine more  
487 accurate yields for  $^{14}\text{C}$  extraction from concrete pyrolysis.

488 The critical discussions of  $^{55}\text{Fe}$  analysis by Leskinen et al. [2] can be summarised in  
489 challenges rising from the low energy decay mode of  $^{55}\text{Fe}$  via electron capture e.g. i)  
490 chemiluminescence exhibits signal in the low LSC channels similar to  $^{55}\text{Fe}$ , ii) the effect  
491 of quenching is especially significant for low energy emissions, and iii) acid tolerance of  
492 the liquid scintillation cocktails. In this study, the relatively high stable Fe content in the  
493 studied activated concrete and the difficulties in the complete destruction of the matrix  
494 caused major difficulties in the  $^{55}\text{Fe}$  analysis.

495 The critical discussions of  $^{63}\text{Ni}$  analysis by Leskinen et al. [2] focused on the importance  
496 of careful removal of  $^{60}\text{Co}$  from the  $^{63}\text{Ni}$  fraction.  $^{60}\text{Co}$  is a prevalent interfering  
497 radionuclide in activated steel whereas it may not be as important in the studied activated  
498 concrete. In this study, no interference by  $^{60}\text{Co}$  in  $^{63}\text{Ni}$  fraction was reported. Most  
499 laboratories implemented a separation on an anion exchange resin in HCl medium to isolate  
500 Ni from Fe. However, as the studied sample contained high amount of Ca, the purified Ni  
501 fraction may have contained also Ca (provided that the preceding hydroxide precipitation  
502 was not performed) since both Ni and Ca are not retained on resin in concentrated HCl  
503 medium and are co-eluted [21]. The presence of high Ca amount hindered the purification  
504 of Ni on Ni resin by precipitating during the loading step of the sample and lowered the  
505 separation yield in comparison to previous works [15].

506 The critical considerations in  $^3\text{H}$  analysis is similar to  $^{14}\text{C}$  analysis as both of them are  
507 volatile radionuclides and pure  $\beta$  emitters. Analysis of this low energy pure  $\beta$  emitter  
508 ( $E_{\text{max}}=18.6$  keV) can be carried out using aqueous leaching, distillation, freeze-drying,  
509 azeotropic distillation, or chemical/thermal oxidative decomposition prior to LSC  
510 measurement [30]. With the exception of oxidative decomposition, quantitative analysis is

511 subject to  $^3\text{H}$  speciation as HTO as the above mentioned methods cannot release strongly  
512 bound  $^3\text{H}$  [30]. For example, studies have shown that in activated concrete  $^3\text{H}$  can be  
513 present in free water (i.e. HTO), in water of crystallisation, in structural OH-groups and be  
514 lattice bound [30]. The lattice bound  $^3\text{H}$  originates mainly from activation of Li impurities  
515 and is the most strongly bound speciation of  $^3\text{H}$  requiring excess of 350 °C temperatures  
516 [30,31]. The loss of  $^3\text{H}$  via evaporation of HTO during storage and sampling can be an  
517 issue in analysis of activated concrete. However, the loss of  $^3\text{H}$  via evaporation can be very  
518 significant in the case of contaminated samples resulting in a negative bias in the  
519 radiochemical analysis. In thermal oxidation methods (i.e. the oxidiser and pyrolyser  
520 utilised in this study),  $^3\text{H}$  needs to be quantitatively released from the solid matrix,  
521 converted to HTO, and trapped into a trapping solution. Therefore, the same challenges  
522 exist with  $^3\text{H}$  as with  $^{14}\text{C}$  analysis discussed by Leskinen et al. [2]. The results submitted  
523 in this study showed excellent consistency even though the analyses were carried out within  
524 a few months' time interval. As such, the storage and sending of the activated concrete  
525 samples had not caused evaporation of  $^3\text{H}$ . On the other hand, it would have been  
526 interesting to compare the thermal oxidation with acid digestion in order to see the  
527 effectiveness of acids to liberate  $^3\text{H}$  from mineral bound position.

528  $^{36}\text{Cl}$  analysis consists of extraction from matrix, its trapping and its purification prior to  
529 LSC measurement. As a volatile DTM radionuclide,  $^{36}\text{Cl}$  has to be released from the matrix  
530 and trapped efficiently. The trapped  $^{36}\text{Cl}$  is then isolated from the interfering radionuclides  
531 (e.g.  $^{129}\text{I}$ ,  $^{99}\text{Tc}$ ) and matrix elements to avoid overestimation and avoid quenching during  
532 LSC measurements. In this intercomparison, the extraction of  $^{36}\text{Cl}$  from the activated  
533 concrete was carried out with acid leaching with 8 M  $\text{HNO}_3$  or with combustion using a  
534 Pyrolyser. In the first case, chloride in the leachate was separated by  $\text{AgCl}$  precipitation  
535 followed by an anion exchange chromatographic purification according to Ref. [23]. The  
536 separated chloride in  $\text{NH}_4\text{Cl}$  solution was then mixed with scintillation cocktail before LSC  
537 analysis. In the second case, the released chlorine was trapped in 6 mM  $\text{Na}_2\text{CO}_3$  medium.  
538 Afterwards,  $^{36}\text{Cl}$  was purified using  $\text{AgCl}$  precipitation and then separated from silver using  
539 anion exchange resin similarly to the first case. The combination of  $\text{AgCl}$  precipitation and  
540 anion exchange resin enabled to achieve decontamination factors higher than  $10^6$  towards  
541 interfering elements such as  $^{129}\text{I}$ ,  $^{35}\text{S}$ ,  $^{14}\text{C}$  or  $^3\text{H}$  and to obtain accurate determination of  $^{36}\text{Cl}$

542 in various matrices [23]. However, the implementation of AgCl precipitation and ion  
543 exchange purifications made  $^{36}\text{Cl}$  analysis lengthy and can induce yield loss, especially for  
544 laboratories that do not perform this analysis routinely or are in the method development  
545 phase, as it was the case of laboratory 8 which observed a 5% yield. Another challenge of  
546  $^{36}\text{Cl}$  determination in the present intercomparison was the very low level of activity  
547 concentration. It was possible to quantify  $^{36}\text{Cl}$  at a very low value of 6 mBq/g by  
548 performing a counting during 10 hours and by leaching a high amount of sample (10 g).  
549 Further investigations have to be carried out to consolidate the  $^{36}\text{Cl}$  determination at low  
550 level. The implementation of AMS measurements or Cl resin (by Eichrom Technologies)  
551 are options to be considered to improve the  $^{36}\text{Cl}$  detection limit.

552  $^{41}\text{Ca}$  analysis includes at least the following features, which require critical considerations.  
553 Success in hydroxide precipitation step, where Fe and Ni are precipitated while Ca should  
554 remain in the solution, is not always complete. Instead, if pH is increased fast with saturated  
555 NaOH to basic pH values, then Ca might precipitate at lower pH and follow Fe and Ni  
556 precipitate to column separation. As discussed in “Overview of the radiochemical  
557 analyses”, this decreases the yield of Ca and complicates column separation of Fe and Ni.  
558 Any interfering beta or x-ray emitting radionuclide in the final purified sample can easily  
559 ruin the LSC spectrum of  $^{41}\text{Ca}$ , due to extremely low energy of x-rays from  $^{41}\text{Ca}$  (0.3-3.6  
560 keV) and their equally poor intensity (strongest emission 7.8%). Although in this work the  
561 concrete matrix did not contain  $^{60}\text{Co}$  at disturbing concentration level, in other cases of  
562 activated concrete  $^{60}\text{Co}$  can be present in higher amounts. In that case,  $^{60}\text{Co}$  should be  
563 removed carefully from the  $^{41}\text{Ca}$  fraction by several repeating precipitations and  
564 monitoring the decontamination progress by gamma measurements of the purified fractions  
565 [17]. Last critical step is dissolution of the evaporation residue containing  $^{41}\text{Ca}$ , either to  
566 HCl or to  $\text{H}_2\text{O}$  prior to adding scintillation cocktail. Regardless of the used solvent, the  
567 produced LSC sample should be clear, without white or other colour precipitate. Chemical  
568 quenching is particularly destructive for  $^{41}\text{Ca}$  samples, combined to fore mentioned low  
569 energy and intensity of  $^{41}\text{Ca}$  x-rays it leads to incredibly low counting efficiency. For  
570 example, sample 7 in this study gave only 2% counting efficiency due to these three factors  
571 together. For standard samples (with no quenching), a higher but still low efficiency value



572 of 7% was obtained, representing the best possible counting efficiency for  $^{41}\text{Ca}$  with this  
573 setup. Therefore, it is essential to eliminate colour quenching from an LSC sample of  $^{41}\text{Ca}$ .

#### 574 *Critical considerations in the gamma emitter analysis*

575 Critical considerations of  $^{60}\text{Co}$  analysis have been discussed by Leskinen et al. [2]. As a  
576 summary, reliable gamma emitter analysis requires properly maintained and calibrated  
577 detector, suitable measurement geometry for the sample size and activity level and  
578 coincidence correction especially with short source-to-detector distance. Additionally, the  
579 most reliable efficiency calibration is possible using experimental measurements with  
580 reference material as close as possible to sample matrix [33]. However, the analysis of  
581  $^{152}\text{Eu}$  is more complicated compared to  $^{60}\text{Co}$ , since  $^{152}\text{Eu}$  decays with electron capture,  
582 positron emission and  $\beta^-$  sending out X-rays (4 photons), betas and gammas (132 photons).  
583 As such  $^{152}\text{Eu}$  has a wide range of peaks which can result in significant true coincidence  
584 summing (TCS). The true coincidence summing occurs also in the case of  $^{60}\text{Co}$  decaying  
585 by emission in cascade 1173 and 1333 keV gamma rays. The size of TCS factor depends  
586 on the measurement geometry, the decay scheme and detector dimensions. Correction  
587 factor of 0.91-1.57 for different energies of  $^{152}\text{Eu}$  has been published in Ref. [34]. In this  
588 intercomparison at VTT, correction factors of 0.96-1.22 for different energies of  $^{152}\text{Eu}$  were  
589 used. In addition to TCS, coincidence summing can also be random coincidence, in which  
590 different nuclei emit radiations (x-rays, annihilation photons and gammas) that are close in  
591 time compared to the detector response time [35]. This phenomenon is more probable at  
592 higher activities and as such, the phenomenon was not significant in this study, because the  
593 samples contained low activities. As a conclusion, if coincidence is not corrected for, the  
594 activity determination of a sample can be significantly underestimated. Therefore,  
595 coincidence summing is a common source of systematic errors in gamma spectrometry.

#### 596 *Critical considerations on uncertainty calculations*

597 Uncertainty calculations were further performed as recommended by Leskinen et al. [2]  
598 and the laboratories were requested to submit further details in their uncertainty

599 calculations. Majority of the provided uncertainties were evaluated according to GUM  
600 method [36]. The calculations were based on the combination of the different sources of  
601 uncertainties. They included measurement uncertainties (e.g. LSC and yield  
602 measurements), uncertainties in the radiochemical analysis (e.g. weights, volumes,  
603 standards, etc.) and uncertainties in the digestion step. It can be underlined that one  
604 laboratory assumed a 10% uncertainty at  $2\sigma$  for the digestion step based on the results  
605 obtained on inactive muds during intercomparison exercises. For one laboratory, only the  
606 counting uncertainty was considered. One laboratory also applied the Kragten numerical  
607 method [37]. Very different values of uncertainties were calculated: for example, for  $^{55}\text{Fe}$ ,  
608 the uncertainties varied from 2.4% up to 160%. Therefore, it can be noticed that the  
609 uncertainty calculations differed from one laboratory to another. The estimation of source  
610 uncertainties is not an easy task to complete. However, the major source of uncertainty  
611 was determined to originate from activity measurement by LSC (measurement statistics  
612 and efficiency curve) whatever the applied method because the activity concentrations  
613 were very low. The other important uncertainties in LSC are due to low energies,  
614 quenching difference related to the difference in chemical compositions of standard used  
615 for calibration and sample, the implementation of TDCR method with HIDEX 300SL  
616 device, the background as well as the scintillator type. Further studies should be carried  
617 out in order to take into account all sources of uncertainties and consolidate their  
618 estimations. The next intercomparison should help to improve the uncertainty evaluation  
619 and to harmonise the practices between laboratories.

### 620 *Critical considerations on limit of detection calculations*

621 The LODs of participating laboratories for  $^{55}\text{Fe}$ ,  $^{63}\text{Ni}$ ,  $^{41}\text{Ca}$  and  $^{14}\text{C}$  were <300 - <500, <90  
622 - <600, <70 - <500 and <40 - < 2500 mBq/g, respectively. The LODs for  $^{55}\text{Fe}$  and  $^{63}\text{Ni}$  are  
623 well below the exemption limits or clearance of materials stated in 2013/59/Euratom  
624 directive, namely 1000 Bq/g for  $^{55}\text{Fe}$  and 100 Bq/g for  $^{63}\text{Ni}$  [38]. For  $^{41}\text{Ca}$ , there is no  
625 exemption limit, due to weak energy and intensity of the x-ray emissions. For  $^{14}\text{C}$ , the  
626 corresponding exemption limit or clearance of materials is 1 Bq/g, which means that part  
627 of the calculated LODs are higher than the exemption limit, although the LODs and

628 exemption limit for  $^{14}\text{C}$  are at the same concentration level. On the other hand, maximum  
629 LOD value of 2.5 Bq/g is still very far from exemption value for the activity concentration  
630 of  $^{14}\text{C}$  in moderate amounts of any type of material, which is 10 000 Bq/g [38].  
631 Nevertheless, disposal of materials which activity concentrations are below LOD needs  
632 still careful attention and comparison of LODs against exemption limits, as this example  
633 points out. The combination of relatively high LOD with relatively low exemption limit  
634 increases the need for optimising radioanalytical separation methods and measurement  
635 techniques for decreasing LOD (e.g. longer measurement time), as well as reassessing the  
636 calculation method for LOD.

637 As the studied activated concrete contained low levels of radioactivities, results below  
638 LOD were expected. This initiated discussion on how the laboratories calculated their LOD  
639 and it was found out that several different calculation methods were used among  
640 participating laboratories. Currie's classical method [39], ISO 11929-1:2019 standard  
641 method [40], French standards NF M60-322 and NF M60-317 [41,42] have been used for  
642 calculating LODs in this work, as well as a simple approach using the value 3 times of the  
643 blank uncertainty in consideration of counting efficiency and chemical recovery. It can be  
644 seen throughout the reported results, that the LOD values have wide variation among  
645 laboratories, often hundred-fold. Because laboratories use firstly different radioanalytical  
646 separation methods, and different measurement methods and instruments and furthermore,  
647 use different calculation methods for producing LODs, comparison of obtained results is  
648 sometimes difficult and the range for LOD values is therefore broad. These considerations  
649 suggest that in the forthcoming intercomparison projects, emphasis should be given to more  
650 uniform practices for calculating, not only LODs, but also uncertainties. In general,  
651 harmonised and ambiguous calculation methods should be taken into use, for facilitating  
652 comparison of results from different laboratories.

## 653 **Conclusions**

654 The second year of intercomparison exercise on DTM analysis in decommissioning waste  
655 can be concluded similarly to the first year, that the analysis of beta-emitter radionuclides

656 in decommissioning waste is difficult especially at very low level. No major difficulty was  
657 observed for the  $^3\text{H}$  analysis as the analysis was carried out using thermal oxidation and  
658 the measured results were in good agreement. In addition, the possible volatility of  $^3\text{H}$   
659 during the project was not observed to cause a bias in the measured results. However,  
660 comparison of the measured  $^3\text{H}$  results ( $55\pm 4 \text{ Bq g}^{-1}$ ) with calculated activity concentration  
661 ( $200\pm 40 \text{ Bq g}^{-1}$ ) showed that loss of  $^3\text{H}$  during sampling, storage and drilling may have  
662 occurred. Additionally, migration of  $^3\text{H}$  within the biological shield could have affected  
663 the results. Low activity level caused difficulties in the  $^{14}\text{C}$  analysis, as the thermal  
664 oxidation was not able to produce results above LOD even though it is a well-established  
665 technique. One laboratory was able to produce a  $^{14}\text{C}$  activity concentration result, which  
666 was relatively well correlated with the calculated result (i.e.  $70\pm 10 \text{ mBq g}^{-1}$  versus  $530\pm 190$   
667  $\text{mBq g}^{-1}$ ) considering the uncertainties in the original chemical composition of nitrogen.  
668 Analysis of  $^{36}\text{Cl}$  was carried out by two laboratories; one well advanced in the  $^{36}\text{Cl}$  analysis  
669 and another in process of  $^{36}\text{Cl}$  method development. A significant difference between the  
670 yields was observed i.e. 5% and over 93%. The only  $^{36}\text{Cl}$  activity concentration result  
671 above LOD correlated well with the corresponding calculated result (i.e.  $6\pm 1 \text{ mBq g}^{-1}$   
672 versus  $23\pm 9 \text{ mBq g}^{-1}$ ). Major difficulties were observed in the  $^{41}\text{Ca}$  analysis as the relatively  
673 easy purification method via precipitations resulted in spectral interferences in LSC  
674 measurements due to possible presence of an interfering radionuclide or severe quenching.  
675 Also, major difficulties were observed in the  $^{55}\text{Fe}$  analysis. The comparison of the  
676 measured  $^{55}\text{Fe}$  activity concentration results above LOD with the corresponding calculated  
677 results showed unacceptable differences ranging from almost 200% up to 13500% higher  
678 measured results most likely due to difficulties in the yield corrections and also due to short  
679 half-life. The analysis of  $^{63}\text{Ni}$  was a quite straightforward process, as no interfering gamma  
680 emitters were observed in the purified fractions. On the other hand, low  $^{63}\text{Ni}$  activity  
681 concentration caused majority of the submitted results to be below LOD. Comparison of  
682 the measured  $^{63}\text{Ni}$  assigned value with the corresponding calculated result (i.e.  $970\pm 380$   
683  $\text{mBq g}^{-1}$  versus  $320\pm 80 \text{ mBq g}^{-1}$ ) showed measured values to be approximately three times  
684 higher, possibly due to overestimated amount of  $^{63}\text{Ni}$  due to spectral interference in  $^{63}\text{Ni}$   
685 determination or different original stable Ni composition in the studied activated samples  
686 and inactive sample, from which the activation calculations were derived.

687 As a conclusion, the second year of the intercomparison exercise project further  
688 strengthened the radiochemical methods for DTM analysis and the participating  
689 laboratories benefitted from the analyses and discussions. The calculation results also  
690 underlined the importance of the input data i.e. in this case the chemical composition and  
691 irradiation history. The calculated results in activated concrete were not as well aligned  
692 with the measured results as in activated steel, because the input data had higher  
693 uncertainties. However, the calculated results in this paper are in a sense more realistic as  
694 majority of the materials in decommissioning projects suffer from conservative  
695 assumptions in the activation calculations.

696 The third year of intercomparison exercise will be on DTM analysis in spent ion exchange  
697 resin. As such, the analyses will be carried out for DTMs originating from both the spent  
698 fuel (e.g.  $^{90}\text{Sr}$ ) and corrosion products (e.g.  $^{55}\text{Fe}$  and  $^{63}\text{Ni}$ ).

## 699 **Acknowledgements**

700 The authors would like to thank the Nordic Nuclear Research NKS-B programme  
701 ([www.nks.org](http://www.nks.org)) for funding the DTM Decom project in which the intercomparison exercise  
702 was carried out. The authors would also like to thank the other participating laboratories,  
703 namely Technical University of Denmark, Cyclife Sweden AB, Fortum Power and Heat  
704 Oy, IFE Kjeller and IFE Halden for provision of data and collaboration. National fundings  
705 were given by Finnish Research Programme on Nuclear Waste Management KYT 2022.  
706 A-LABOS-EX-PR-SC-01 project is thanked for the CEA self-funding. The authors would  
707 also like to thank FiR1 decommissioning personnel for the provision of studied material  
708 and collaboration.

## 709 **References**

- 710 1. Leskinen A, Tanhua-Tyrkkö M, Kekki T, Salminen Paatero S, Zhang W, Hou X,  
711 Stenberg Bruzell F, Suutari T, Kangas S, Rautio S, Wendel C, Bourgeaux-Goget M,  
712 Stordal S, Isdahl I, Fichet P, Gautier C, Brennetot R, Lambrot G, Laporte E (2020).

- 713 Intercomparison exercise in analysis of DTM in decommissioning waste. NKS-429,  
714 NKS-B, Roskilde, Denmark
- 715 2. Leskinen A, Salminen Paatero S, Gautier C, Rätty A, Tanhua-Tyrkkö M, Fichet P,  
716 Kekki T, Zhang W, Bubendorff J, Laporte E, Lambrot G, Brennetot R (2020).  
717 Intercomparison exercise on difficult to measure radionuclides in activated steel:  
718 statistical analysis of radioanalytical results and activation calculations, J Radioanal  
719 Nucl Chem, 324:1303-1316
- 720 3. International Standard ISO 13528:2015(E) (2015) Statistical methods for use in  
721 proficiency testing by interlaboratory comparison. J Radioanal Nucl Chem 324:1303-  
722 1316
- 723 4. Leskinen A, Tanhua-Tyrkkö M, Salminen Paatero S, Laurila J, Kurhela K, Hou X,  
724 Stenberg Bruzell F, Suutari T, Kangas S, Rautio S, Wendel C, Bourgeaux-Goget M,  
725 Moussa J, Stordal S, Isdahl I, Gautier C, Laporte E, Guiliani M, Bubendorff J, Fichet  
726 P (2021). DTM-Decom II - Intercomparison exercise in analysis of DTM in  
727 decommissioning waste. NKS-441, NKS-B, Roskilde, Denmark
- 728 5. Kotiluoto P, Rätty A (2016) FiR 1 activity inventories for decommissioning planning.  
729 VTT Research report series, VTT-R-03599-16
- 730 6. Gauld I C, Radulescu G, Ilaş G, Murphy B D, Williams M L (2011) Isotopic Depletion  
731 and Decay Methods and Analysis Capabilities in SCALE. Nucl Technol, 174:169-195
- 732 7. Rätty A, Kekki T, Tanhua-Tyrkkö M, Lavonen T, Myllykylä E (2018) Preliminary Waste  
733 Characterization Measurements in FiR 1 TRIGA Research Reactor Decommissioning  
734 project. Nucl Technol 203(2):205-220
- 735 8. Rätty A, Lavonen T, Leskinen A, Likonen J, Postolache C, Fugaru V, Bubueanu G,  
736 Lungu C, Bucsa A (2019) Characterization measurements of fluental and graphite in  
737 FiR1 TRIGA research reactor decommissioning waste. Nucl Eng Design 353:110198
- 738 9. Rätty A (2020) Activity characterisation studies in FiR1 TRIGA research reactor  
739 decommissioning project, Doctoral school in natural sciences dissertation series,  
740 URN:ISSN:2670-2010
- 741 10. X-5 Monte Carlo Team (2003) MCNP – A General Monte Carlo N-Particle Transport  
742 Code, Version 5, Los Alamos National Laboratory, LA-UR-03-1987

- 743 11. Rätty A, Kotiluoto P (2016) FiR 1 TRIGA Activity Inventories for Decommissioning  
744 Planning, Nucl Technol, 194:28-38
- 745 12. Beckurts KH, Wirtz K (1964) Neutron Physics, Appendix I 407-416, Springer-Verlag  
746 Berlin Heidelberg
- 747 13. Leskinen A, Salminen-Paatero S, Rätty A, Tanhua-Tyrkkö M, Iso-Markku T, Puukko  
748 E (2020) Determination of  $^{14}\text{C}$ ,  $^{55}\text{Fe}$ ,  $^{63}\text{Ni}$  and gamma emitters in activated RPV steel  
749 samples - a comparison between calculations and experimental analysis. J Radioanal  
750 Nucl Chem 323:399-413
- 751 14. Gautier C, Laporte E, Lambrot G, Giuliani M, Colin C, Bubendorff J, Crozet M,  
752 Mougél C (2020) Accurate measurement of  $^{55}\text{Fe}$  in radioactive waste. J Radioanal Nucl  
753 Chem, 326:591-601
- 754 15. Gautier C, Colin C, Garcia C (2015) A comparative study using liquid scintillation  
755 counting to determine  $^{63}\text{Ni}$  in low and intermediate level radioactive waste. J Radioanal  
756 Nucl Chem, 308:261-270
- 757 16. Eichrom Method (2014) Nickel-63/59 in water, No NIW01 analytical procedure  
758 revision 1.3
- 759 17. Ervanne H, Hakanen M, Lehto J, Kvarnström R, Eurajoki T (2009) Determination of  
760  $^{45}\text{Ca}$  and  $\gamma$ -emitting radionuclides in concrete from a nuclear power plant. Radiochim  
761 Acta, 97:631-636
- 762 18. Hou X (2005) Rapid analysis of  $^{14}\text{C}$  and  $^3\text{H}$  in graphite and concrete for  
763 decommissioning of nuclear reactor. Appl Radiat Isotop 62:871-882
- 764 19. Hou XL, (2005) Radiochemical determination of  $^{41}\text{Ca}$  in reactor concrete for  
765 decommissioning, Radiochim Acta, 93:611-617
- 766 20. Hou X. (2018) Analytical procedure for simultaneous determination of  $^{63}\text{Ni}$  and  $^{55}\text{Fe}$ .  
767 NKS-B RadWorkshop
- 768 21. Hou X, Østergaard L.F., Nielsen S.P. (2005a) Determination of  $^{63}\text{Ni}$  and  $^{55}\text{Fe}$  in nuclear  
769 waste samples using radiochemical separation and liquid scintillation counting. Anal  
770 Chim Acta 535(1-2): 297-307

- 771 22. Hou X.L., Østergaard L.F., Nielsen S.P. (2005b) Determination of  $^{63}\text{Ni}$  and  $^{55}\text{Fe}$  in  
772 nuclear waste and environmental samples. *Anal Chim Acta* 535:297-307
- 773 23. Hou, X.L., Østergaard L.F., Nielsen S.P. (2007). Determination of  $^{36}\text{Cl}$  in Nuclear  
774 Waste from Reactor Decommissioning. *Anal Chem* 79:3126-3134
- 775 24. Itoh, M., Watanabe, K., Hatakeyama, M., Tachibana, M., (2002) Determination of  $^{41}\text{Ca}$   
776 in biological-shield concrete by low-energy X-ray spectrometry, *Anal Bioanal Chem*  
777 372:532-536
- 778 25. Nottoli, E., Bourles, D., Bienvenu, P., Labet, A., Arnold, M., Bertaux, M., (2013)  
779 Accurate determination of  $^{41}\text{Ca}$  concentrations in spent resins from the nuclear industry  
780 by accelerator Mass spectrometry, *Appl Rad Isot* 82:340-346
- 781 26. Triskem International method, (2013) Cl-36/I-129 separation, TKI – CL01 – V-  
782 1.4\_EN.
- 783 27. Kojima, S., Furukawa, M. (1985) Liquid Scintillation Counting of  $^{55}\text{Fe}$  Applied to Air-  
784 filter Samples. *Radioisot* 34:72-77
- 785 28. Priya S, Gopalakrishnan RK, Goswami A (2014) TDCR measurements of  $^3\text{H}$ ,  $^{63}\text{Ni}$   
786 and  $^{55}\text{Fe}$  using Hidex 300SL LSC device. *J Radioanal Nucl Chem* 302:353-359
- 787 29. NRG Petten, nuclear reaction program TALYS, <http://www.talys.eu/home/> (accessed  
788 on 5.8.2019)
- 789 30. Kim JK, Warwick PE, Croudace IW (2008) Tritium speciation in nuclear reactor  
790 bioshield concrete and its impact on accurate analysis. *Anal Chem* 80:5476-5480
- 791 31. Warwick PE, Kim D, Croudace IW, Oh J (2010) Effective desorption of tritium from  
792 diverse solid matrices and its application to routine analysis of decommissioning  
793 materials. *Anal Chim Acta* 676:93-102
- 794 32. Brennetot R, Giuliani M, Guégan S, Fichet P, Chiri L, Deloffre P, Masset A, Mougél  
795 C, Bachelet F (2017)  $^3\text{H}$  measurement in radioactive wastes: Efficiency of the pyrolysis



- 796 method to extract tritium from aqueous effluent, oil and concrete. Fusion Sci Technol  
797 71:397-402
- 798 33. Harms A, Gilligan C (2010) Development of a neutron-activated concrete powder  
799 reference material. Appl Rad Isot 68:1471-1476
- 800 34. Rodenas J, Gallardo S, Ortiz J (2007) Comparison of a laboratory spectrum of  $^{152}\text{Eu}$   
801 with results of simulation using the MCNP code. Nucl Instrum Methods A 580:303-305
- 802 35. Shweikani R, Hasan M, Takeyeddin M (2013) A simplified techniques to determine  
803 random coincidence summing of gamma rays and dead time count loss corrections.  
804 Appl Radiat Isotop 82:72-74
- 805 36. BIPM, IEC, IFCC, ISO, IUPAC, IUPAP and OIML, "Guide to the expression of  
806 Uncertainty in Measurement", 2nd ed., JCGM, 2008
- 807 37. Kragten J (1994) Calculating Standard Deviations and Confidence Intervals with a  
808 Universally Applicable Spreadsheet Technique. Analyst 119:2161-2165
- 809 38. 2013/59/Euratom directive. [https://eur-lex.europa.eu/legal-](https://eur-lex.europa.eu/legal-content/EN/TXT/?uri=CELEX%3A32013L0059)  
810 [content/EN/TXT/?uri=CELEX%3A32013L0059](https://eur-lex.europa.eu/legal-content/EN/TXT/?uri=CELEX%3A32013L0059)
- 811 39. Currie LA (1968). Limits for qualitative detection and quantitative determination.  
812 Application to radiochemistry. Anal Chem 40(3): 586-593
- 813 40. International Standard ISO 11929-1:2019, Determination of the characteristic limits  
814 (decision threshold, detection limit and limits of the coverage interval) for  
815 measurements of ionizing radiation – Fundamentals and application – Part 1:  
816 Elementary applications
- 817 41. NF M60-322 (2005) Technologie du cycle du combustible nucléaire – Déchets –  
818 Détermination de l'activité du fer 55 dans les effluents et déchets par scintillation  
819 liquide, après séparation chimique préalable. Association Française de Normalisation,  
820 Paris, France.

821 42. NF M60-317 (2001) Technologie du cycle du combustible – Déchets – Détermination  
822 de l'activité du nickel 63 dans les effluents et déchets par scintillation liquide, après  
823 séparation chimique préalable. Association Française de Normalisation, Paris, France.